J. Membrane Biol. 157, 147–158 (1997)

The Journal of
Membrane
Biology

Inositol Polyphosphates Modify the Kinetics of a Small Chloride Channel in Skeletal Muscle Sarcoplasmic Reticulum

J.I. Kourie[1], P.S. Foster[2], A.F. Dulhunty[1]

[1]Muscle Research Group, Division of Neuroscience, Division of Biochemistry and Molecular Biology, John Curtin School of Medical Research, Australian National University, P.O. Box 334, Canberra City, ACT 2601, Australia

[2]Cellular Signal Transduction Group, Division of Biochemistry and Molecular Biology, John Curtin School of Medical Research, Australian National University, P.O. Box 334, Canberra City, ACT 2601, Australia

Received: 19 August 1996/Revised: 23 December 1996

Abstract. The actions of D-*myo*-inositol 1,4,5-trisphosphate (IP_3) and D-*myo*-inositol 1,3,4,5-tetrakisphospate (IP_4) on small chloride (SCl) channels from rabbit skeletal muscle sarcoplasmic reticulum are reported. We find that the inositol polyphosphates (6–40 μM) are potent reversible blockers of SCl channels in lipid bilayers at −40 mV with $>10^{-5}$ M *cis* (cytoplasmic) Ca^{2+} when added to the *cis*, but not *trans*, chamber. IP_3 or IP_4 at 20 μM reduced the mean open time from 89 ± 16 msec to 11 ± 2 msec or to 8.0 ± 1.0 msec respectively, by abolishing the longest time constant component in the open time distribution. Neither IP_3 nor IP_4 altered the six single-channel conductance levels. The fraction of low conductance events increased ~4-fold and the dwell time at the lower conductance levels increased ~3-fold. Channel gating was altered so that most transitions were between the closed level and an open level, in contrast to control channels which remained open for long periods with many transitions between the six open levels. The actions of the inositol polyphosphates were: (1) not prevented by 20 μg/ml *cis* heparin (an IP_3 receptor blocker); (2) mimicked by 10 μM *cis* synthetic inositol polyphosphates, L-*chiro*-inositol 1,4,6-trisphosphate and L-*chiro*-inositol 1,4,6-trisphosphorothionate (which do not bind to IP_3 receptors); (3) mimicked by *cis* additions of the polyanions heparin or hepran (20 μg/ml each) and vanadate (500 μM). The results suggest that an interaction between polyanions and SCl channels would allow the channels to be modulated in vivo by inositol polyphosphates.

Key words: Sarcoplasmic reticulum — Small chloride channels — Skeletal muscle — Inositol phosphates — Polyanions — Submaximal conductance levels

Introduction

A variety of cation channels are activated or blocked by inositol polyphosphates (*see* e.g., Berridge, 1993). For example, D-*myo*-inositol 1,4,5-trisphosphate (IP_3) mobilizes Ca^{2+} from endoplasmic reticulum (ER) stores by activating the IP_3 receptor (IP_3R) Ca^{2+} release channel (Bezprozvanny & Ehrlich, 1994). IP_3, by releasing Ca^{2+} from the ER, has the potential to indirectly activate Ca^{2+}-activated anion and cation channels in the plasmalemma and in internal membranes (e.g., Evans & Marty, 1986; Reeves & Gurich, 1994; Latorre, Vergara, & Hidalgo, 1982). In addition, it has recently been discovered that IP_3 and D-*myo*-inositol 1,3,4,5-tetrakisphospate (IP_4) interact directly with, to activate or block, cation channels other than the IP_3R in plasmalemma and nuclear membranes (Berridge, 1993; Malvivya, 1994). IP_4 prevents the activation of Cl^- secretion by epithelial cells in response to an increase in cytoplasmic [Ca^{2+}] (Vajanaphanich et al., 1994). Although the mechanism for this effect is unknown, it has been suggested that IP_4 may bind to Cl^- channels in the epithelial plasmalemma and block their Ca^{2+} activation mechanism (Kachintorn et al., 1993). Inositol polyphosphates have not previously been shown to directly activate or block anion channels.

Neither IP_3-activated nor IP_3-blocked single ion channels have been reported in mammalian skeletal muscle sarcoplasmic reticulum (SR) membranes (Foster, 1994), although pathways for inositol polyphosphate metabolism are localized in the transverse (T-) tubule membrane (Hidalgo et al., 1993) and IP_3 increases myoplasmic [Ca^{2+}] under some conditions (Vergara, Tsien, & Delay, 1985). The mechanism for the increase in cytoplasmic [Ca^{2+}] is obscure since the fast-glycolytic fibers used in these experiments contain few IP_3Rs (Moschella

et al., 1995) and IP_3 does not cause significant activation of the ryanodine receptor (RyR) Ca^{2+} release channels in mammalian skeletal muscle (Foster, 1994; Valdivia et al., 1990; Valdivia et al., 1992). Therefore the IP_3-induced increase in cytoplasmic [Ca^{2+}] may be mediated by effects of IP_3 on other mechanisms which facilitate an increase in cytoplasmic Ca^{2+}, either by enhancing Ca^{2+} release and/or blocking the Ca^{2+} uptake, e.g., SR ion channels—like the small chloride (SCl) channel—which could provide counter ion pathways during Ca^{2+} release or uptake by the SR.

The recently described SCl channel, in contrast to other types of Cl^- channel in skeletal SR, is regulated by factors which may vary during excitation-contraction coupling, including SR membrane potential and cytoplasmic [Ca^{2+}] (Kourie et al., 1996*a,b*). The SCl channel is anion selective, with a slope conductance of 65–75 pS, (250/50 mM Cl^-, *cis/trans*) and is characterized by prominent activity to 6 submaximal conductance levels and by voltage-dependent activation, inactivation and deactivation properties. The channel is maximally active for several seconds after voltage pulses to potentials between −20 to −40 mV and then it inactivates after a period of seconds at −40 to −80 mV, or minutes at 0 to −20 mV. Inactivation is relieved by 0.5 to 1.0-sec pulses to positive potentials. Thus the SCl channel is more active at the negative membrane potentials that may be achieved during Ca^{2+} uptake by the SR (Yu, Hao, & Inesi, 1994), and when cytoplasmic [Ca^{2+}] is 10^{-5} M or higher (Kourie et al., 1996*a*). Therefore it has been suggested that a major function of the channel might be charge compensation during Ca^{2+} uptake (Kourie et al., 1996*a,b*). In this case the SCl channel function would be analogous to that of anion channels in the ER, which are essential for optimal Ca^{2+} uptake and Ca^{2+} ATPase activity (Beyerdorffer et al., 1984; Kemmer et al., 1987). If the SCl channel is essential for optimal Ca^{2+} uptake by the SR, then blockers of its activity would reduce Ca^{2+} uptake and lead to an increase in cytoplasmic [Ca^{2+}], which could induce further Ca^{2+} release via Ca^{2+}-activation of the RyR (Thastrup et al., 1990).

In the present study we have explored the possibility that IP_3 blocks SCl channels, and explored the possible mechanisms of such a block. Inhibitory effects of IP_3 and IP_4 on the SCl channel are described, as well as the actions of two synthetic inositol polyphosphates, L-*chiro*-inositol-1,4,6, trisphosphate (L-*chr* Ins(1,4,6)P_3) and the phosphothioate, L-*chiro*-inositol 1,4,6-trisphosphorothionate (L-*chr* Ins(1,4,6)PS_3), which do not mobilize Ca^{2+} stores or displace IP_3 from the IP_3R (Safrany et al., 1991). The interactions between heparin or vanadate and IP_3/IP_4 were examined. Heparin is a specific inhibitor of IP_3 binding to the IP_3R and of IP_3-induced Ca^{2+} mobilization (Ghosh et al., 1988) and decavanadate also prevents Ca^{2+} mobilization from ER by IP_3 (Föhr et al., 1991). The results show that IP_3 and IP_4, at physiological concentrations (20 μM), reduce the mean current flowing through the channel (i.e., block the channel) by reducing channel open times, and replacing openings to the maximum conductance with openings to submaximal conductance levels, when added to the *cis* (cytoplasmic), but not the *trans* (luminal), side of the channel. IP_3 and IP_4 do not bind to a ''classical'' IP_3R because their actions: (a) are seen with *cis* [Ca^{2+}] of 1 mM, (b) are not prevented by heparin, and (c) are reproduced by L-*chr* Ins(1,4,6)P_3 and L-*chr* Ins(1,4,6)PS_3. All polyanions tested had similar inhibitory effects on SCl channel activity and their actions were additive. We suggest that the inositol polyphosphates block the SCl channel by binding to a polyanion specific site on the channel. A part of the action of IP_3 in increasing cytoplasmic [Ca^{2+}] in skeletal muscle may be mediated by IP_3 binding to this polyanion specific site, thus blocking the SCl channel and reducing Ca^{2+} uptake by the SR. The results provide evidence for a novel mechanism for inositol polyphosphate regulation of SR function, i.e., by blocking an anion channel in the SR membrane.

Materials and Methods

The methods for preparation of SR vesicles, bilayer formation and analysis of single-channel data have been described previously (Kourie et al., 1996*a,b*) and are briefly outlined.

Preparation of SR Vesicles

SR vesicles were prepared from back and leg muscles of New Zealand rabbits. Longitudinal SR and terminal cisternae vesicles were collected from bands at specific density interfaces of a discontinuous sucrose gradient. The vesicles were frozen and stored in liquid N_2. Band 2 (B2) vesicles contained mostly longitudinal SR and band 4 (B4) vesicles contained mostly terminal cisternae SR; contamination of both bands with outer mitochondrial membrane is less than 3%.

Bilayer Cups, Lipid Bilayers and Vesicle Fusion

Bilayers were formed across an aperture (150 μm in diameter) in the wall of 1 ml delrin® cups, using a mixture of palmitoyl-oleoyl-phosphatidylethanolamine, palmitoyl-oleoyl-phosphatidylserine and palmitoyl-oleoyl-phosphatidylcholine (5:3:2, by volume), obtained in chloroform from Avanti Polar Lipids (Alabaster, Alabama). The lipid mixture was dried under N_2 and redissolved in *n*-decane at a final concentration of 50 mg/ml.

The formation of the lipid bilayer was detected from its total capacitance which was measured from the current response to a voltage ramp ranging from 0 to −140 mV in 140 msec (1 *V*/sec, the ''bilayer test;'' Kourie, 1996). B2 and B4 vesicles were added to a final protein concentration of 1–10 μg/ml. SCl channels were incorporated in similar numbers from both vesicle fractions. The side of the bilayer to which vesicles were added is defined as *cis*, the other side as *trans.* It was assumed that the cytoplasmic side of the SR membrane faced the *cis* chamber and this has been confirmed in our B4 vesicles.

Solutions for Bilayers

Solutions contained choline Cl (250 mM *cis*/50 mM *trans*), plus 1 mM $CaCl_2$ and 10 mM HEPES (pH 7.2, adjusted with NaOH). Stock solutions (0.1 to 1.0 mM) were prepared by addition of IP_3, IP_4, L-*chr* Ins(1,4,6)P_3, L-*chr* Ins(1,4,6)PS_3, heparin, hepran and vanadate to the *cis* solution. L-*chr* Ins(1,4,6)P_3 and L-*chr* Ins(1,4,6)PS_3 were synthesized from L-quebrachitol and purified by ion exchange chromatography on DEAE-sepharose and used as triethylammonium salts (Safrany et al., 1991). Vanadate stock solutions were prepared freshly before each experiment and used within two hours of preparation. Na_3VO_4 was dissolved in the *cis* solution at pH 7.4. The solution had the orange color indicative of the presence of decavanadate ($Na_6V_{10}O_{28}$) (Neumcke & Weik, 1991).

Recording and Analysis of Single-Channel Data

Voltage was controlled and current recorded with an Axopatch 200 amplifier (Axon Instruments). Potentials are given with respect to the *trans* chamber. The *cis* and *trans* chambers were connected to the amplifier headstage by Ag/AgCl electrodes in agar salt-bridges containing the solutions present in each chamber. Current was monitored on an oscilloscope, stored on video tape using pulse code modulation (PCM-501; Sony Corp.) and later filtered at 1 kHz (−3dB, 4-pole bessel) and digitised with a TL-1 DMA interface (Tecmar) at 2 kHz. Experiments were done at 20–25°C.

Two analysis programs were used. An in-house analysis program, CHANNEL 2 (developed by P.W. Gage and M. Smith), was used to measure the following overall parameters of channel activity: mean open time, T_o (i.e., the total time that the channel was not closed and including openings to all conductance levels, divided by the length of the record); frequency of opening, F_o; the open probability, P_o (i.e, the sum of all open times as a fraction of the total time); the integral of the current divided by the total time; i.e., the mean current, I'. Since measurements of open times and P_o included openings to submaximal conductance levels, the threshold for channel opening or closing was normally set at 1.5 times the baseline noise, i.e., between −0.4 and −0.6 pA (the maximum current at −40 mV was about −6 pA). This level, rather than a 50% discriminator, was used so as to include the many openings to submaximal conductance levels that were less than 50% of the maximum conductance (Kourie et al., 1996*a*). Records were further filtered for Channel2 analysis and display using a running average of 3 to 5 data points or a Gaussian filter of 200Hz.

The program EVPROC (kindly provided by Dr. D.R. Laver) was used for analysis of single-channel conductance levels. A detailed description and evaluation of EVPROC is given in Kourie et al. (1996*a*). Briefly, EVPROV assumed that the channel activity consists of a series of step transitions between stationary conductance levels. The program produced a signal consisting of current levels and transitions between levels. Current levels are the mean of data points between transitions. Transitions are steps, *T*, in which:

$$(T/\sqrt{n}) > 2\ I_{RMS}$$

where *n* is smallest number of samples in the levels before and after the transition and, I_{RMS} is the root mean squared of the noise obtained from sections of the record in which the channel was closed. Event amplitude histograms (Fig. 5*A* and *B*), event duration histograms (Fig. 6*A*) and transition matrices (Fig. 6*C* and *D*) were compiled directly from the idealized signal. The mean durations of events at each amplitude (Fig. 5*C* and *D*) were calculated by dividing the total number samples by the number of events at each amplitude. EVPROC was also set to analyze channel open durations (Fig. 6*D*). An opening was defined as a transition from the closed level between 0 pA and −0.5 pA to a level at, or more negative than, −0.5 pA. The channel was considered to remain open until the current dropped to a level between −0.5 and 0 pA. The durations of all events within the open period were summed to obtain durations of the openings, which were compiled into open duration histograms.

Average results are given as mean ± 1 SEM. The Students' *t*-test was used to test the significance of differences between average data from normal channels and average data from polyanion-treated channels. A P value of ≤ 0.05 was considered significant.

Results

Effects of IP_3 and IP_4 on SCl Channel Activity

IP_3 (6–40 μM) had no visible effect on inactive SCl channels at 10^{-7} M *cis* Ca^{2+} ($n = 2$), but blocked active channels at −40 mV with *cis* $Ca^{2+} > 10^{-5}$ M, when added to the *cis* ($n = 10$), but not *trans* ($n = 2$), chamber. SCl channels were fully active between 10^{-5} M and 10^{-3} M *cis* Ca^{2+} (Kourie et al., 1996*a*) and the action of IP_3 was independent of [Ca^{2+}] with this range. Most results were obtained using 10^{-3} M *cis* Ca^{2+}, which was used to encourage vesicle fusion with the bilayer, and at a bilayer potential of −40 mV during the several seconds that they were active after prepulses to positive potentials (Fig. 1*A*). All channels showed bursts of activity at −40 mV for periods (*t*) of ~10 to 30 sec after the prepulse, before inactivation induced long closures lasting 10 sec to many mins (Fig. 1*A*). The maximum conductance was ~75 pS and the channel opened to several substates levels (Fig. 1*A* and *C*).

Addition of *cis* IP_3 and IP_4 (6 to 37.5 μM) abbreviated channel openings (Fig. 1*B* and *D*) and the time (*t*) that activity continued after the prepulse was lengthened, usually within ~10 sec of addition of *cis* IP_3 or IP_4. Channel activity slowly reversed to the normal pattern after perfusion with IP_x-free solution. Fig. 1*E* shows a partial recovery of activity, 92 sec after IP_3-washout. Full recovery in 7 channels was seen within 120 to 320 sec of IP_4 washout.

Concentration-dependence of Inositol Polyphosphate Action

Channel activity (including bursts and interburst intervals) was analyzed during the first 5 sec after the prepulse, within period *t* (Fig. 1). Although the maximum changes in activity were, on average, essentially the same with IP_3 and with IP_4, the half maximum concentrations were generally lower with IP_4 (Fig. 2). The changes in mean open time (T_o) and event frequency (F_o) were maximal between 5–12 μM IP_x (Fig. 2*A* and *B*), while the reduction in P_o and mean current (I') continued up to 25 μM IP_x (Fig. 2*C* and *D*). These differences

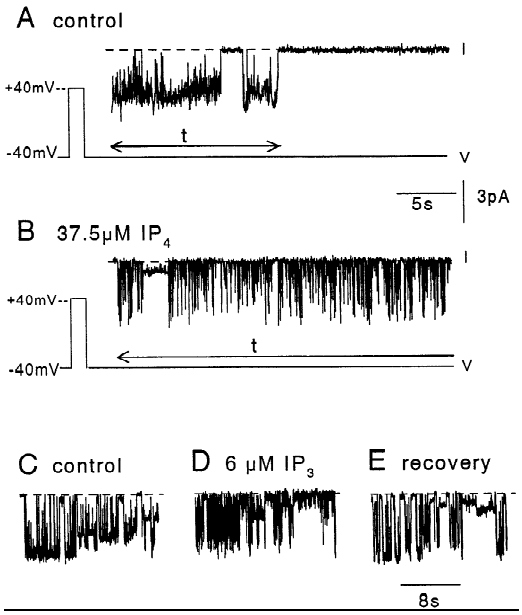

Fig. 1. Activity of SCl channels is altered by IP_4 or IP_3 addition to the *cis* chamber. In this and subsequent figures: single channel records (*I*) were obtained at −40 mV with 250/50 mM choline Cl *cis/trans*, the broken lines indicate closed current levels and channel opening is downward (inward current). (*A*) Control activity after a prepulse to +40 mV, with two bursts of activity, separated by a 1.8-sec closure and followed by closure that lasted 46 sec before the bilayer was subjected to another prepulse. (*B*) The same channel after addition of 37.5 μM IP_4. Channel activity continued for 33 sec after the prepulse: the first 29 sec are shown. Continuous lines in *A* and *B* indicate bilayer potential (*V*). The arrow (*t*) indicates the duration of activity after the prepulse. (*C*) Control activity in a second channel. (*D*) The same channel 70 sec after *cis* addition of 6 μM IP_3. (*E*) 92 sec after the *cis* perfusion with drug-free solution.

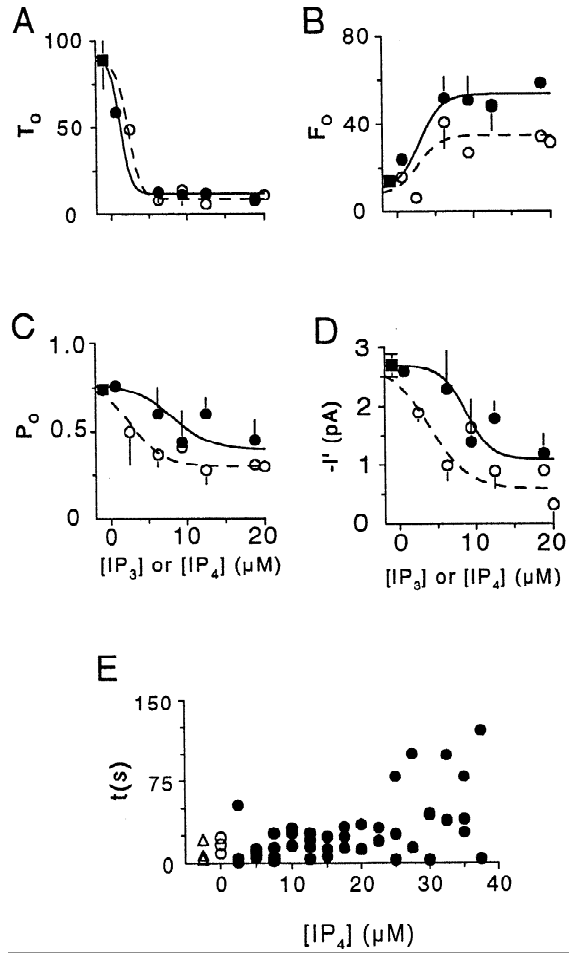

Fig. 2. Analysis of mean open time (T_o) in *A*, frequency of opening (F_o) in *B*, open probability (P_o) in *C* and mean current (I') in *D*, from channels exposed to IP_3 (filled circles, $n = 5$) or IP_4 (open circles, $n = 7$). Data at one to three different concentrations of IP_x were obtained from each channel. Controls (filled squares at $[IP_x] = 0$) are the average of the 12 channels. Each point for channels exposed to IP_x (filled and open circles) is the mean of data from two to five channels. 5 sec of activity after 3–5 voltage pulses was analyzed for each channel. Vertical bars on the data points show ±1 SEM. The average T_o, F_o, P_o, and I' were significantly different from normal ($P < 0.01$) at each $[IP_4] > 5.0$ μM. The increase in T_o and decrease in P_o were significant ($P < 0.05$) only at 18.8 μM IP_3, the increase in F_o and decrease in I' were significant ($P < 0.05$) with $[IP_3] > 6.3$ μM. (*E*) The duration of bursting activity after the prepulse (*t*) in seconds in one channel under control conditions, before addition of *cis* IP_4 (open circles), after washout of IP_4 (open triangles), and after addition of increasing concentrations of IP_4 (filled circles).

reflect the complex effects of IP_3 on SCl channel gating to maximal and submaximal conductance levels (below). When parameters for all $[IP_3] > 6$ μM were lumped together (Table 1), each was significantly different from control ($P < 0.01$).

The periods of channel activation after the voltage pulse, with interburst intervals less than 10 sec (*t*, Fig. 1 above), measured with higher $[IP_4]$s were outside the range of times seen under control conditions (Fig. 2*E*), in each channel with $[IP_x] > 10$ μM.

Inositol Polyphosphates Alter Open-Time Distributions

The distribution of all open and closed times, within the 5-sec interval after the prepulses, were analyzed in plots of √frequency of events in logged bins (Sigworth & Sine, 1987) to compare the wide range of durations and display the exponential time constants as peaks in the distribution. Control open times fell into three exponential components (Fig. 3*B*), in contrast to openings after addition of IP_4, which fell into two components with time constants (Fig. 3*D*) similar to τ_{o1} and τ_{o2} in control.

On average (Fig. 3*E* and *F*), most control openings (open symbols) were in τ_{o3}. The fraction of openings in this longest component was reduced by *cis* IP_3/IP_4 (filled

Table 1. Average values for mean open time (T_o), frequency of opening (F_o), P_o and mean current (I') obtained from eleven control channels, 5 channels exposed to IP_3 and 7 channels exposed to IP_4, at concentrations between 6 and 40 μM. Data are shown as mean ± SEM.

	T_o	F_o	P_o	I'
Control	89.2 ± 15.9	13.8 ± 1.8	0.74 ± 0.04	−2.5 ± 0.2
IP_3	11.2 ± 1.9**	53.2 ± 3.1**	0.53 ± 0.07*	−1.8 ± 0.3*
IP_4	8.4 ± 1.4**	40.2 ± 5.7**	0.29 ± 0.04**	−0.7 ± 0.2**

* indicates a difference from control with P < 0.01
** indicates a difference from control with P < 0.0005
Differences in mean values were considered significant if P < 0.05

symbols, P < 0.0005). The closed time distributions were not significantly altered after addition of IP_3 or IP_4 (Fig. 3*G* and *H*).

SCl Channel Openings to Substate Levels

Substate levels were commonly seen in SCl channel activity and occupied a greater fraction of the activity as [IP_3] and [IP_4] increased. Six nonzero current levels form peaks in the all-points histograms for control and recovered recordings (Fig. 4*A* and *C*) and in the presence of IP_4 (Fig. 4*B*).

Most control openings were to the maximum conductance or to submaximal levels greater than 50% of maximum (levels 4, 5 and 6). In contrast to control, most activity in the presence of IP_4 was to levels less than 50% of the maximum conductance (levels 1, 2 and 3). Channel openings to the maximum conductance recovered when IP_4 was removed (Fig. 4*C*). The increase in activity to low conductance levels was maximal at ~20 μM IP_4 (Fig. 4*D* and *E*).

Analysis of Conductance Levels in the Presence and Absence of IP_4

The amplitude and dwell times of events were further analysed using the program EVPROC (Materials and Methods). As with the all points histograms of the raw data (Fig. 5), the conductance levels were the same in the absence (Fig. 5*A*) and presence (Fig. 5*B*) of IP_4, but there is a marked increase in the fraction of events to conductance levels of <2 pA with the inositol polyphosphate.

The mean dwell time at the larger conductance levels was ~3 msec under both control and IP_4 conditions (Fig. 5*C* and *D*). However, the dwell times at the smaller conductance levels (<2 pA), *increased* from ~2 msec under control conditions to ~11 msec in the presence of IP_4.

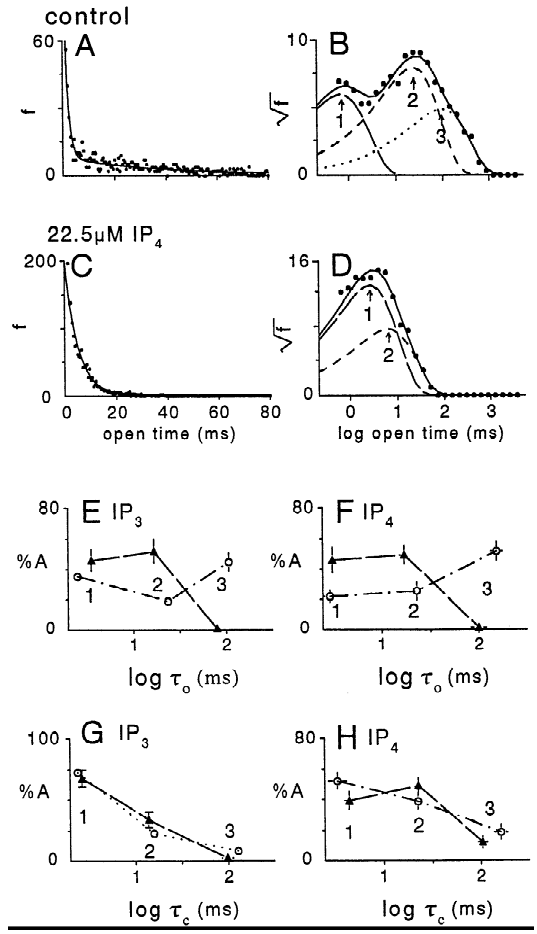

Fig. 3. Effects of *cis* IP_3/IP_4 on open and closed time distributions. (*A–F*) Open-time histograms for a single channel before (*A* and *B*), and after exposure to 22.5 μM IP_4 (*C* and *D*). Histograms on the left are frequency (*f*) of openings in 0.5 msec bins (*A* and *C*) and those on the right are the square root of frequency (√f) of openings in logged bins (7/decade, *B* and *D*). Continuous lines (*A–D*)—the best least squares fit of a multiple exponential function to the log-binned data. Broken lines (*B* and *D*)—individual exponentials curves, with peaks corresponding to the time constants. *E* and *F* show the mean percentage of openings (%*A*) plotted against mean time constants of each component (τ_{on}), on a log scale. *G* and *H* show results of a similar analysis of closed-time distributions: the mean percentage of closures (%*A*) is plotted against the mean time constant of each component ($\tau_c n$). In *E–H:* open circles show control values and filled triangles show average values for 0.6–37.5 μM IP_x. Numbers (1,2 and 3) in the log-binned histograms (arrows, *B* and *D*) and in graphs of average data (*E–H*) indicate time constants of the first, second and third components respectively (i.e., τ_{o1}, τ_{o2} τ_{o3} or τ_{c1}, τ_{c2} τ_{c3}). Vertical bars show ±1 SEM of the %*A*. Horizontal bars show ±1 SEM of $\tau_o n$ or $\tau_c n$, where the SEM is greater than the dimensions of the symbol.

The basic action of inositol polyphosphates on channel gating is illustrated in the dwell time and open duration histograms (Fig. 6*A* and *B*) and in the transition analyses (Fig. 6*C* and *D*).

The time constants in the distribution of dwell times

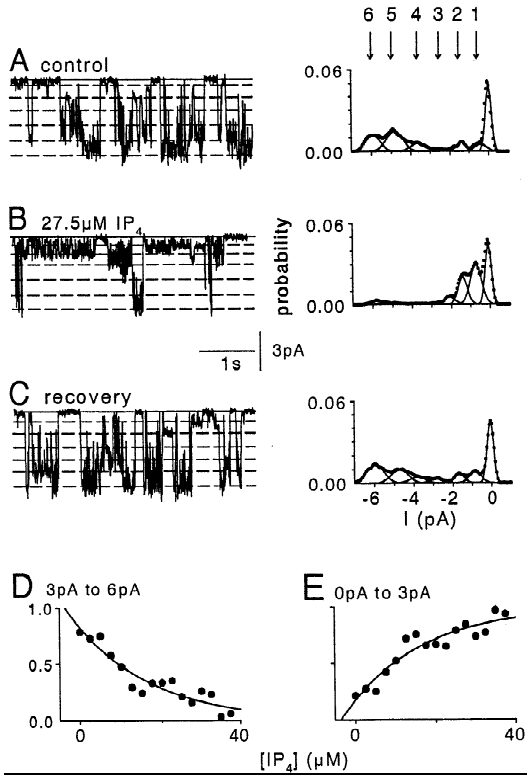

Fig. 4. Increased transitions to submaximal conductance levels in SCl channels in the presence of *cis* IP_4. The left hand panel contains selected data showing openings to submaximal conductance levels and the right hand panel contains all points histograms of data in the adjacent record (filled circles). (*A*) Control; (*B*) in the presence of 27.5 μM IP_4; (*C*) following perfusion of the *cis* chamber with drug-free solution. The curves through the data in the histogram are the best fit of a multiple Gaussian function with peaks indicating conductance levels (arrows indicate the six peaks which were the same in the three histograms). The broken lines through the records on the left show conductance levels indicated by the peaks in the corresponding multiple Gaussian distribution. The continuous lines indicate the zero current levels. (*D*) The fraction of channel activity to high conductance levels—in Gaussian curves with peaks between −3 pA and −6 pA. (*E*) The fraction of channel activity to low conductance levels—in Gaussian curves with peaks between zero and −3 pA. Sections of records lasting 60 to 200 sec were analyzed at each [IP_4] to obtain the data points in *D* and *E*.

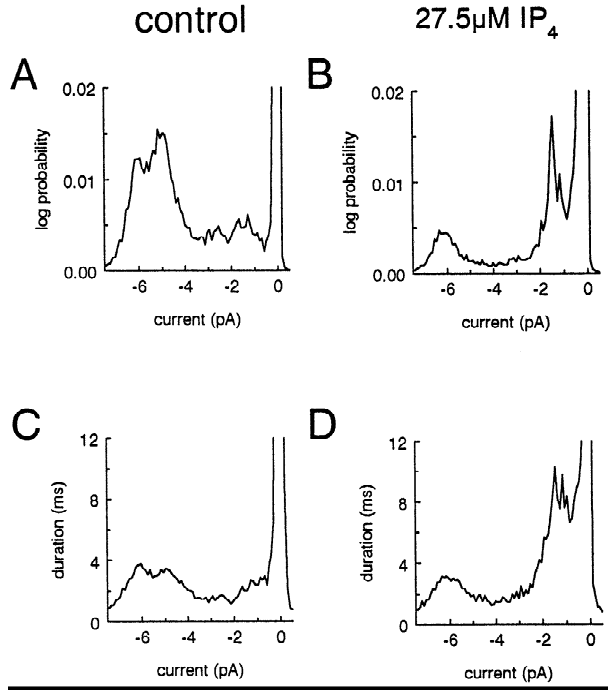

Fig. 5. The effect of 27.5 μM *cis* IP_4 on the probability and duration of current amplitudes, determined by EVPROC analysis of ~140 sec (280,000 data points) of control channel activity, and 137 sec of activity with 27.5 μM *cis* IP_4, from the SCl channel shown in Fig. 4. The control activity was that obtained before addition of IP_4 plus that obtained after IP_4 washout. (*A*) control probability distribution. (*B*) probability distribution with 27.5 μM *cis* IP_4. (*C*) Mean duration of control current amplitudes. (*D*) Mean duration of current amplitudes with 27.5 μM *cis* IP_4. Probability distributions were obtained from normalized frequency distributions generated by EVPROV. Mean duration was derived from EVPROC analysis by dividing the number of data points at each level by the number of events at each level.

(τ_{d1} – τ_{d4}, Table 2) were similar under control conditions (Fig. 6*A*, open symbols) and with IP_4 (Fig. 6*A*, filled symbols). The increased fraction (%A, Table 2) of dwell times of 10–100 msec (τ_{d3}) with IP_4 reflect the longer sojourns at low conductance levels (Fig. 5*D* above). Durations of channel openings (periods during which the channel was not closed and the current remained more negative than −0.5 pA, Materials and Methods) showed a very different pattern (Fig. 6*B*, Table 2), similar to the results of Channel2 analysis of the raw data (Fig. 3 *above*). Most control openings were in a long time constant component (τ_{o3}) at ~200 msec. In contrast, with IP_4, most openings were in the two shorter components (τ_{o1} and τ_{o2}), with time constants of ~12 and ~54 msec. Note that dwell times >1000 msec (τ_{d4}, Fig. 6*A*) were to current levels between 0 and −0.5 pA and were not detected in the open duration analysis (Fig. 6*B*) because the minimum current for an opening was set a −0.5 pA (*above*).

The majority of control transitions were between high conductance levels and lower levels and form the dark bins near the diagonal in the transition diagram: few transitions were from an open level to the closed state (Fig. 6*C*). Thus the channel was open for long periods during which it underwent many transitions between different levels. In contrast to control, the IP_4-modified channel opened to each conductance level from the closed state, and then returned to the closed state before reopening: the darker bins (with higher numbers of transitions) are near the axes and away from the diagonal (Fig. 6*D*). The same changes in amplitude, dwell times,

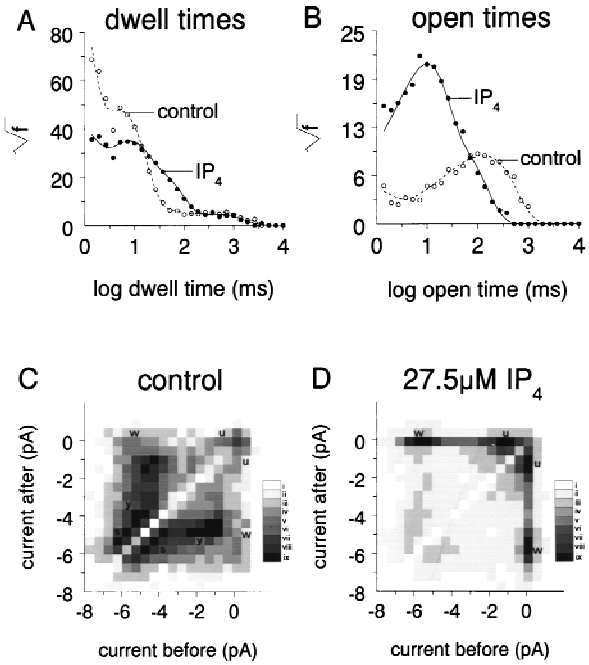

Fig. 6. Channels gating determined by EVPROC analysis of the same sections of data analysed for Fig. 5. Control data was obtained before addition of IP_4 and after IP_4 washout. (*A*) Dwell time histograms. (*B*) Open duration histograms (Materials and Methods). Control data (open circles, broken lines) and data with 27.5 μM *cis* IP_4 (filled circles, continuous lines) are shown on each histogram. Curves in *A* and *B* are best least squares fits of a multiple exponential function to the data. The time constants and percentage of dwell times and durations in each exponential component are given in Table 2. *C* and *D* are gray-scale diagrams of transitions between maintained current levels. Squares (bins) below the diagonal show the frequency of transitions to a larger (more negative) current amplitude. Squares above the diagonal show transitions to a smaller (more positive) current amplitude. (*C*) Control. Darker regions near the diagonal (*s*) indicate a high frequency of transitions between larger current levels (−5 pA to −6 pA). Darker region near the baseline (*u*) shows transitions between levels near the baseline. There are frequent transitions between the baseline and levels at −4 pA to −6 pA (*w*) and between substates in the −2 pA to −4 pA range (*y*). (*D*) 27.5 μM IP_4. A simpler gating pattern than the control, with few transitions between substate levels. Most transitions between the baseline and levels between −4 pA and −6 pA (*w*) or between the baseline and levels between 0 pA and −2 pA (*u*). The numerals beside the gray scales indicate the following numbers of transitions. In *C:* i, 0; ii, 1–2; iii, 3–9; iv, 10–16; v, 16–22; vi, 22–31; vii, 31–43; viii, 43–60; ix, >60. In *B:* i, 0; ii, 1–8; iii, 9–25; iv, 26–72; v, 73–101; vi, 102–143; vii, 144–203; viii, 204–288; ix, >288.

open durations and transitions were seen in the 15 channels exposed to IP_3 and IP_4.

The Voltage-dependence of SCl Channel Gating

Voltage-dependence was not systematically examined with IP_3 or IP_4, but was measured in 2 channels exposed to L-*chr* Ins(1,4,6)P_3 whose action was identical to that of IP_3/IP_4 (*below*). Although P_o was reduced at all potentials after addition of L-*chr* Ins(1,4,6)P_3, the bell-shaped relationship between P_o and membrane potential remained. P_o increased from low values at positive potentials to maximum values at ~−35 mV and then decreased at more negative potentials. The voltage-dependent increase in P_o, in the absence and presence of L-*chr* Ins(1,4,6)P_3 was due to the parallel increases in the mean open time and frequency of openings previously reported (Kourie et al., 1996*b*).

The Mechanism of the Inositol Polyphosphate Effect on SCl Channel Gating

The effects of IP_3 and IP_4 could have been mediated by inositol polyphosphate binding to:

(1) a ''classical'' IP_3R which is functionally coupled to SCl channels in the SR membrane;

(2) an inositol polyphosphate-specific site on the SCl channel, or a closely associated protein;

(3) a polyanion specific site on the SCl channel, or on a closely associated protein.

The following experiments with heparin and two IP_3 analogues were performed to distinguish between these possibilities.

Heparin

IP_3/IP_4 binding and activation of IP_3Rs and IP_3/IP_4-activated plasmalemmal channels are antagonized by heparin (Berridge, 1993; Vaca & Kunze, 1995). In contrast 20 μM *cis* IP_4, added after 20 μg/ml *cis* heparin, produced an additive effect on SCl channels (Fig. 7*A*). This additive effect was also seen when heparin was added in the presence of 20 μM IP_4 (*not shown*). Unexpectedly, addition of heparin alone (Fig. 7*A*) had a similar reversible action to that seen with IP_3/IP_4. Similar results were obtained in 3 channels (Table 3).

L-*chr* Ins(1,4,6)P_3 and L-*chr* Ins(1,4,6)PS_3

These analogues of IP_3 do not interact with IP_3 occupancy of IP_3Rs or Ca^{2+} mobilization by IP_3 (Introduction). However, both analogues altered SCl channel activity (Fig. 7*B* & Table 3) in a similar way to IP_3/IP_4. This observation together with the finding that heparin also mimicked the IP_3/IP_4 effect indicate that inositol polyphosphates do not block SCl channels via an IP_3R.

SCl Channel Gating is Altered in the Same Way by Several Polyanions

The polyanions hepran (20 μg/ml) and vanadate (500 μM) acted in a similar manner to the inositol polyphos-

Table 2. Time constants for dwell times (τ_{dn}) and open durations (τ_{on}) in msec obtained from the best least squares fit of a multiple exponential function to dwell times and open durations obtained from EVPROC analysis of single channel data shown in Fig. 6. The percentage of dwell times and open durations (%A) in each exponential component are given in parentheses.

	τ_{d1} (A)	τ_{d2} (A)	τ_{d3} (A)	τ_{d4} (A)	τ_{o1} (A)	τ_{o2} (A)	τ_{o3} (A)
			msec (%)			msec (%)	
Control	0.6 (82)	6.8 (17)	45 (0.3)	700 (0.2)	1.0 (17)	60 (17)	200 (66)
IP_4	0.8 (49)	9.0 (34)	39 (14)	600 (0.6)	12.5 (81)	54 (19)	

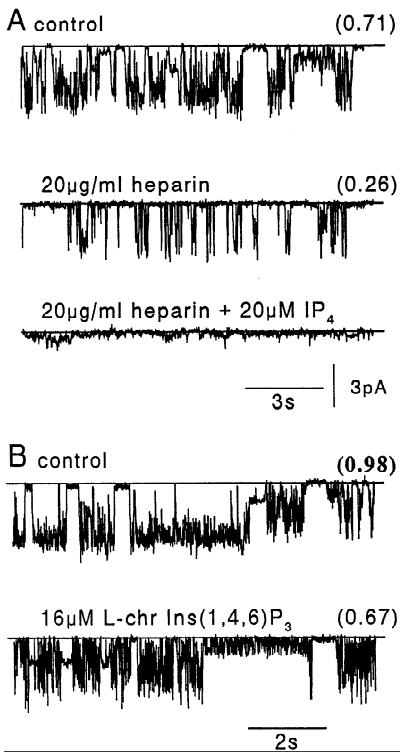

Fig. 7. Actions of heparin and the synthetic analogue of IP_3 on SCl channel activity. (*A*) Heparin does not antagonize the effects of IP_4 on SCl channel activity. The upper panel shows control channel activity; the second panel shows activity obtained 120 sec after *cis* addition of 20 μg/ml heparin; the third panel shows activity recorded when 20 μM IP_4 was added to the *cis* chamber 170 sec after the heparin—the record was obtained after 50 sec with heparin + IP_4. (*B*) L-*chr* Ins(1,4,6)P_3 mimics IP_3 effects. The upper panel shows control activity and the second panel shows activity in the same channel 72 sec after *cis* addition of 16 μM L-*chr* Ins(1,4,6)P_3.

phates and heparin (Table 3). On average, there were trends towards a reduction in mean open time, an increase in the frequency of opening, and a decrease in P_o and mean current (Table 3). The changes were statistically significant in most individual channels ($P < 0.005$). The polyanions generally decreased the fraction of events in the longest component of the open-time distributions (Fig. 8), with little change in the closed time distributions (not shown).

Table 3. Mean open time (T_o), frequency of opening (F_o), open probability (P_o) and mean current (I') obtained with *cis* application 10 μM L-*chr* Ins(1,4,6)P_3 (IP_{146}, $n = 3$), 10 μM L-*chr* Ins(1,4,6)PS_3 (SIP_{146}, $n = 2$), 20 μg/ml heparin ($n = 3$), 20 μg/ml hepran ($n = 1$) and 500 μM vanadate ($n = 1$). When $n > 1$, the values presented are the mean ± SEM of the means obtained in each channel from analysis of 5-sec sections of activity after 3 to 5 voltage pulses. When $n = 1$, the values presented are the mean ± SEM of values obtained from analysis of 4 to 5 of such 5-sec sections of activity.

	T_o	F_o	P_o	I'
Control	118.1 ± 22.3	8.7 ± 1.2	0.69 ± 0.06	−2.1 ± 0.2
IP_{146}	10.6 ± 1.5*	28.4 ± 6.8**	0.31 ± 0.09*	−0.8 ± 0.3*
SIP_{146}	10.0 ± 0.6*	22.8 ± 6.8**	0.25 ± 0.04**	−1.4 ± 0.3
Heparin	33.8 ± 7.6	13.6 ± 2.9	0.37 ± 0.03*	−1.4 ± 0.2*
Hepran	44.8 ± 2.3	12.3 ± 0.1	0.55 ± 0.03	−1.2 ± 0.1*
Vanadate	23.7 ± 1.3*	21.9 ± 0.6**	0.50 ± 0.02	−1.1 ± 0.1*

* indicates that the data is significantly different from control with $P < 0.05$

** indicates that the data is significantly different from control with $P < 0.005$

In addition, all polyanions increased channel opening to low conductance substate levels (e.g., Fig. 7). Analysis with EVPROC showed an increase in the number and dwell times of events to low substate levels, reduction in the duration of channel openings and increased numbers of transitions between the baseline and all levels in channels modified by the polyanions (*data not shown*). These changes were again the same as those seen with IP_3 and IP_4.

Discussion

We describe a potent blocking action of IP_3 and IP_4 on the SCl channel in skeletal muscle SR. The inositol polyphosphates, at physiological concentrations, reduce the mean current flowing through the channel. This action is not induced by inositol polyphosphate binding to an ''IP_3 receptor'' since the effect of IP_3 is not blocked by heparin or by vanadate (*see below*). It is likely that IP_3 and IP_4 bind to a general polyanion binding site on the SCl channel or on a coprotein in the SR since several difference polyanions, including the IP_3 analogues, have

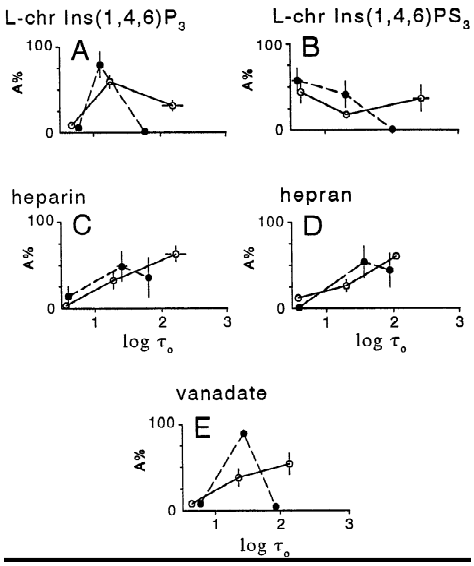

Fig. 8. Effects of five different polyanions on the open time distributions of 10 single SCl channels. (*A*) Average of three channels exposed to 10 μM L-*chr* Ins(1,4,6)P_3. (*B*) Average of two channels exposed to 10 μM L-*chr* Ins(1,4,6)PS_3. (*C*) Average of three channels exposed to 20 μg/ml heparin. (*D*) One channel exposed to 20 μg/ml heparin. (*E*) One channel exposed to 500 μM vanadate. When $n > 1$, the values presented are the mean ± SEM of the means obtained in each channel from analysis of 5-sec sections of activity after 3-to-5 voltage pulses. When $n = 1$, the values presented are the mean ± SEM of values obtained from analysis of 4 to 5 such 5 sec sections of activity. The open and closed times were analyzed in the same way as those in Fig. 3, in graphs of the square root of frequency of events in logged bins. The average results are displayed in the same way as the average results in Fig. 3*E*. The vertical bars show ±1 SEM of the mean percentage of closures, and the horizontal bars show ±1 SEM of the mean time constant, where these are greater than the dimensions of the symbol.

a similar action on SCl channel activity. Adenosine phosphates (0.5 mM) block SCl channel activity in much the same way, with a potency that reflects their negative charge density: $ATP^{4-}/ATPH^{3-} > ADP^{3-} >>> AMP^{2-}$ (Kourie, 1997; G.P. Ahern, *unpublished observations*). However anions with a lower negative charge density, e.g., HPO_4^{2-} (250 mM *cis* or *trans*, $n = 4$, D.R. Laver, J.I. Kourie & A.F. Dulhunty, *unpublished observations*), and SO_4^{2-} up to 70 mM (Kourie et al., 1996*b*), do not alter SCl channel gating.

Inositol Polyphosphate and Polyanion-mediated Effects on Ion Channels

Direct actions of inositol polyphosphates, and the other polyanions examined here, on Cl^- channels have not previously been reported, although there is an interaction between IP_3/IP_4 and Cl^- secretion (*see* Introduction). In contrast, there are several reports of inositol polyphosphates directly activating or inhibiting cation channels. For example, IP_3 and IP_4 stimulate voltage-dependent K^+ currents (Wu et al., 1991) and activate Ca^{2+} channels in plasmalemma and nuclear membranes (*see below*). RyR channels are activated by phosphatidylinositol 4,5-bisphosphate (Chu & Stefani, 1991) and some amphibian RyRs are activated by IP_3 (Suarez-Isla et al., 1991). Histamine-induced K^+ currents in smooth muscle, and cerebellar K^+ channels, are inhibited by IP_4 (Molleman et al., 1991; Timerman et al., 1992). In addition, cation channels are activated by other polyanions; polysulfates increase RyR activity (Bezprozvanny et al., 1993), heparin increases L-type Ca^{2+} currents (Knaus et al., 1990) and vanadate activates ATP-sensitive K^+ channels (Neumcke & Weik, 1991). This activation of cation channels by polyanions contrasts with the block of the anion channel reported here.

The Response of SCl Channels to IP_3 and IP_4 Differs from that of Most Cation Channels

The response of the SCl channel to IP_3 and IP_4 differs from that reported for other single ion channels in several significant ways.

(1)''Classical'' IP_3Rs are either not activated by IP_4, or are far less sensitive to IP_4 (Wilcox et al., 1993), while the SCl channel is equally sensitive to IP_3 and IP_4.

(2) Activation of IP_3Rs, and IP_3/IP_4 receptors in plasmalemma and nuclear membranes, by IP_3/IP_4 is inhibited by heparin (Ghosh et al., 1988; Malvivya, 1994; Vaca & Kunze, 1995), whereas heparin mimics, and is additive with, IP_4 in blocking SCl channels.

(3) Activation of IP_3Rs by IP_3 is blocked by decavandate (Föhr et al., 1991), while vanadate (containing decavanadate, Materials and Methods) mimics SCl channel block by IP_3/IP_4.

(4) The synthetic analogues of IP_3, which do not bind to the IP_3R (Safrany et al., 1991), reduce the current flowing through the SCl channel in the same way as IP_3/IP_4.

(5) IP_3/IP_4 activate most cation channels by increasing the frequency and duration of channel openings (Bezprozvanny, Watras, & Ehrlich, 1991; Vaca & Kunze, 1995), while the block of SCl channels depends partly on a reduction in the duration of channel openings.

When inositol polyphosphate receptor K^+ channels from the cerebellum are blocked by IP_4 (Chadwick et al., 1992), the mean open time is reduced. However, in contrast to the block of the SCl channel, the block of the cerebellar K^+ channel is specific for IP_4 (i.e., it is not seen with IP_3) and does not involve openings to subconductance levels.

Subconductance Activity in SCl Channels

A characteristic property of SCl channels is the frequent opening to substates with 6 conductance levels. The syn-

chronization gating of channel openings to the maximum conductance and to submaximal conductance levels is exquisitely sensitive to cytoplasmic [Ca^{2+}] (Kourie et al., 1996*a*), to polyanions and inositol polyphosphates (this study), and to adenosine polyphosphates (Kourie, 1997; G.P. Ahern, *unpublished observations; see* Results). Therefore the current flowing through SCl channels in vivo must be critically dependent on the functional and metabolic state of the fiber.

Mechanism of Polyanion Block of SCl Channels: Stabilization of Subconductance Levels

The block of SCl channels was associated with (a) fewer long openings and (b) fewer openings to the maximum conductance, but increased activity to submaximal conductance states.

The shift in channel activity towards submaximum conductance states has not previously been identified as a blocking mechanism. Reduced conductances are associated with ''fast block'' and with Mg^{2+} block of K^+ channels (Hille, 1992), with voltage-dependent block and with QX314 block of ryanodine receptors (Hille, 1992; Tinker & Williams, 1993). However in each case, and in contrast to polyanion block of SCl channels, the lower conductance levels are introduced by the blocking drug and are seen rarely, if at all, in normal channel activity.

Subconductance states in channel activity could reflect the unsynchronized gating of current through several conducting pores within the protein (Krouse, Schneider, & Gage, 1986). One hypothesis is that the polyanions uncouple the normal partial synchronization of SCl channel gating so that channel openings to all conductance levels are from the closed state, openings to the maximum conductance become infrequent and openings to subconductance states dominate activity. The redistribution of channel activity towards subconductance states suggests that the polyanions interrupt channel gating mechanisms, rather than simply blocking the channel pore.

The briefer channel openings induced by the polyanions is reminiscent of ''flicker block'' of K^+ channels by Cs^+ or QX222 block of cholinergic channels (*see* e.g., Hille, 1992). However, the polyanion block of SCl channels appears to have unique characteristics in that new brief time constants are not introduced into the open time distributions and channel dwell times at individual conductance levels are not reduced. The polyanions specifically eliminate the longest time constant component of the open time distribution and, in contrast to flicker block, increase dwell times at the lower submaximal conductance levels.

The polyanion binding site appears to be on the cytoplasmic side of the channel and is presumably not located on the transmembrane segments of the protein, since the effects are not voltage-dependent. Increasing [polyanion] (this study), or decreasing [Ca^{2+}] (Kourie et al., 1996*a*), have similar effects in increasing substate activity and, in the extreme, both abolish channel activity. The coordination of SCl channel activity may depend on a high positive charge density on the cytoplasmic surface of the protein: a reduction in this positive charge could lead to fewer openings to the maximum conductance and, eventually, to cessation of channel openings.

The Role of SCl Channels in Striated Muscle

SCl channels have been identified in skeletal muscle (Kourie et al., 1996*a*,*b*) and similar Cl^- channels have been described in cardiac muscle (Decrouy, Juteau, & Rousseau, 1995; Townsend & Rosenberg, 1995). Although the specific function of the channels is yet to be identified, they are likely to maintain charge balance across the SR membrane during Ca^{2+} release and/or reuptake. SCl channels may also provide a functional communication between T-tubule membranes which release IP_3 (Hidalgo et al., 1993) and terminal cisternae and longitudinal SR membranes which contain the SCl channels. The activation of contraction by IP_3 in skeletal muscle (Vergara et al., 1985) could depend on the IP_3 block of the SCl channel if the channel was essential for counterion flow during Ca^{2+} uptake by the SR in vivo, since channel block would reduce Ca^{2+} uptake and lead to an increase in myoplasmic [Ca^{2+}], which may itself activate Ca^{2+} release via the RyR (Thastrup et al., 1990), and induce contraction. The suggested role of the SCl channels in Ca^{2+} uptake by the SR is similar to the demonstrated role of anion channels in ATP-dependent Ca^{2+} transport in ER (Beyerdorffer et al., 1984; Kemmer et al., 1987). The blocking action of IP_3 on the SCl channel may also play a role in elevation of myoplasmic [Ca^{2+}] in malignant hyperthermia (MH), since IP_3 levels are higher than normal in muscle from MH susceptible pigs (Foster et al., 1989).

In conclusion, we show that several polyanions, including IP_3 and IP_4 at physiological concentrations, reduce the mean current flowing through SCl channels by reducing the average time that the channels are open and by reducing the number of openings to the maximum conductance. The polyanions apparently induce these effects by interacting with the channel gating mechanisms, not by simple channel block. The differential sensitivity of the subconductance levels to intracellular messengers, like Ca^{2+} and inositol polyphosphates, provides a novel mechanism for regulation of the current flowing through ion channels.

We thank Professor B.V.L. Potter, School of Pharmacy and Pharmacology and Institute for Life Sciences, University of Bath, Bath, England, for supplying the structural analogues of IP_3. We thank Professor P.W. Gage and Dr. D.R. Laver for their comments on the manuscript and Dr. D.R. Laver for his assistance with EVPROC. We are

indebted to Suzie Pace and Joan Stivala for their excellent assistance and for preparation and characterization of SR vesicles.

References

Berridge, M.J. 1993. Inositol trisphosphate and calcium signalling. *Nature* **361:**315–325

Beyerdorffer, E., Streb, H., Eckhardt, L., Haase, W., Schulz, I. 1984. Characterization of calcium uptake into rough endoplasmic reticulum of rat pancreas. *J. Membrane Biol.* **81:**69–82

Bezprozvanny, I., Ehrlich, B.E. 1994. Inositol (1,4,5)-trisphosphate ($InsP_3$)-gated Ca channels from cerebellum: conduction properties for divalent cations and regulation by intraluminal calcium. *J. Gen. Physiol.* **104:**821–856

Bezprozvanny, I.B., Ondrias, K., Kaftan, E., Stoyanovsky, D.A., Ehrlich, B.E. 1993. Activation of the calcium release channel (ryanodine receptor) by heparin and other polyanions is calcium dependent. *Mol. Biol. Cell* **4:**347–352

Bezprozvanny, I., Watras, J., Ehrlich, B.E. 1991. Bell-shaped calcium-response curves of $Ins(1,4,5)P_3$- and calcium-gated channels from endoplasmic reticulum of cerebellum. *Nature* **351:**751–754

Chadwick, C.C., Timerman, A.P., Saito, A., Mayrleitner, M., Schindler, H., Fleischer, S. 1992. Structural and functional characterization of an inositol polyphosphate receptor from cerebellum. *J. Biol. Chem.* **267:**3473–3481

Chu, A., Stefani, E. 1991. Phosphatidylinositol 4,5-Bisphosphate-induced Ca^{++} release from skeletal muscle sarcoplasmic reticulum terminal cisternal membranes. *J. Biol. Chem.* **266:**7699–7705

Decrouy, A., Juteau, M., Rousseau, E. 1995. Examination of the role of phosphorylation and phospholamban in the regulation of the cardiac sarcoplasmic reticulum Cl^- channel. *J. Membrane Biol.* **146:**315–326

Evans, M.G., Marty, A. 1986. Calcium-dependent chloride currents in isolated cells from rat lacrimal glands. *J. Physiol.* **378:**437–460

Föhr, K.J., Wahl, Y., Engling, R., Kemmer, T.P., Gratzl, M. 1991. Decavanadate displaces inositol 1,4,5-tris-phosphate (IP_3) from its receptor and inhibits IP_3 induced Ca^{++} release in permeabilized pancreatic acinar cells. *Cell Calcium* **12:**735–742

Foster, P.S. 1994. The role of phosphoinositide metabolism in Ca^{++} signalling of skeletal muscle cells. *Int. J. Biochem.* **26:**449–468

Foster, P.S., Gesini, E., Claudianos, C., Hopkinson, K.C., Denborough, M.A. 1989. Inositol 1,4,5,-trisphosphate phosphatase deficiency and malignant hyperpyrexia in swine. *Lancet* **July 15:**124–127

Ghosh, T.K., Eis, P.S., Mullaney, J.M., Ebert, C.L., Gill, D.L. 1988. Competitive, reversible, and potent antagonism of Inositol 1,4,5-Trisphosphate-activated calcium release by heparin. *J. Biol. Chem.* **263:**11075–11079

Hidalgo, C., Jorquera, J., Taipa, V., Donoso, P. 1993. Triads and transverse tubules isolated from skeletal muscle contain high levels of inositol 1,4,5-trisphosphate. *J. Biol. Chem.* **268:**15111–15117

Hille B. 1992. Ionic channels of excitable membranes. Hille B, editor. 2nd ed: Sinauer Associates; Sunderland, MA

Kachintorn, U., Vajanaphanich, M., Barrett, K.E., Traynor-Kaplan, A.E. 1993. Elevation of inositol tetrakisphosphate parallels inhibition of Ca^{++}-dependent Cl^- secretion in T84 cells. *Am. J. Physiol.* **264:**C671–C676

Kemmer, T.P., Bayerdorffer, E., Will, H., Schulz, I. 1987. Anion dependence of Ca^{2+} transport and (Ca^{2+} + K^+)-stimulated Mg^{2+}-dependent transport ATPase in rat pancreatic endoplasmic reticulum. *J. Biol. Chem.* **262:**13758–13764

Knaus, H.-G., Scheffauer, F., Romanin, C., Schindler, H.-G., Glossmann, H. 1990. Heparin binds with high affinity to voltage-dependent L-type Ca^{++} channels. *J. Biol. Chem.* **265:**11156–11166

Kourie, J.I. 1996. Vagaries of artificial bilayers and gating modes of the SCl channel from the sarcoplasmic reticulum of skeletal muscle. *J. Membr. Sci.* **116:**221–227

Kourie, J.I. 1997. ATP-sensitive voltage- and calcium-dependent chloride channels in sarcoplasmic reticulum vesicles from rabbit skeletal muscle. *J. Membrane Biol.* **156** (*in press*)

Kourie, J.I., Laver, D.R., Ahern, G.P., Dulhunty, A.F. 1996*a*. A calcium-activated chloride channel in sarcoplasmic reticulum vesicles from rabbit skeletal muscle. *Am. J. Physiol.* **270:**C1675–C1686

Kourie, J.I., Laver, D.R., Junankar, P.R., Gage, P.W., Dulhunty, A.F. 1996*b*. Characteristics of two types of chloride channel in sarcoplasmic reticulum vesicles from rabbit skeletal muscle. *Biophys. J.* **70:**202–221

Krouse, M.E., Schneider, G.T., Gage, P.W. 1986. A large anion-selective channel has seven conductance levels. *Nature* **319:**58–60

Latorre, R., Vergara, C., Hidalgo, C. 1982. Reconstitution in planar lipid bilayers of a Ca^{++}-dependent K^+ channel from transverse tubule membranes isolated from rabbit skeletal muscle. *Proc. Natl. Acad. Sci. USA* **79:**805–809

Malvivya, A.N. 1994. The nuclear inositol 1,4,5-trisphosphate and inositol 1,3,4,5-tetrakisphosphate receptors. *Cell Calcium* **16:**301–313

Molleman, A., Hoiting, B., Duin, M., van den Akker, J., Nelemans, A., Dn Hertog, A. 1991. Potassium channels regulated by inositol 1,3,4,5-tetrakisphosphate and internal calcium in DDT1MF-2 smooth muscle cells. *J. Biol. Chem.* **266:**5658–5663

Moschella, M.C., Watras, J., Jayaraman, T., Marks, A.R. 1995. Inositol 1,4,5-trisphosphate receptor in skeletal muscle: differential expression in myofibres. *J. Muscle Res. Cell Motil.* **16:**390–400

Neumcke, B., Weik, R. 1991. Vanadate as an activator of ATP-sensitive potassium channels in mouse skeletal muscle. *Eur. Biophys. J.* **19:**119–123

Reeves, W.B., Gurich, R.W. 1994. Calcium-dependent chloride channels in endosomes from rabbit kidney cortex. *Am. J. Physiol.* **266:**C741–C750

Safrany, S.T., Wojcikiewicz, R.J.H., Strupish, J., McBain, J., Cooke, A.M., Potter, B.V.L., Nahorski, S.R. 1991. Synthetic phosphorothioate-containing analogues of inositol 1,4,5-trisphosphate mobilize intracellular Ca^{++} stores and interact differentially with inositol 1,4,5-trisphosphate 5-phosphatase and 3-kinase. *Mol. Pharmacol.* **39:**754–761

Sigworth, F.J., Sine, S.M. 1987. Data transformations for improved display and fitting of single-channel dwell time histograms. *Biophys. J.* **52:**1047–1054

Suarez-Isla, B.A., Alcayaga, C., Marengo, J.J., Bull, R. 1991. Activation of inositol trisphosphate-sensitive Ca^{++} channels of sarcoplasmic reticulum from frog skeletal muscle. *J. Physiol.* **441:**575–591

Thastrup, O., Cullen, P.J., Drobak, B.K., Hanley, M.R., Dawson, A.P. 1990. Thapsigargin, a tumor promotor, discharges intracellular Ca^{2+} stores by specific inhibition of the endoplasmic reticulum Ca^{2+}-ATPase. *Proc. Natl. Acad. Sci. USA* **87:**2466–2470

Timerman, A.P., Mayrleitner, M.M., Lukas, T.J., Chadwick, C.C., Saito, A., Watterson, D.M., Schindler, H., Fleischer, S. 1992. Inositol polyphosphate receptor and clathrin assembly protein AP-2 are related proteins that form potassium-selective ion channels in planar lipid bilayers. *Proc. Natl. Acad. Sci. USA* **89:**8976–8980

Tinker, A., Williams, A.J. 1993. Charged local anesthetics block ionic conduction in the sheep cardiac sarcoplasmic reticulum calcium release channel. *Biophys. J.* **65:**852–864

Townsend, C., Rosenberg, R.L. 1995. Characterization of a chloride channel reconstituted from cardiac sarcoplasmic reticulum. *J. Membrane. Biol.* **147:**121–136

Vaca, L., Kunze, D.L. 1995. IP_3-activated Ca^{++} channels in the plasma membrane of cultured vascular endothelial cells. *Am. J. Physiol.* **269:**C733–C738

Vajanaphanich, M., Schultz, C., Rudolf, M.T., Wasserman, M., Enyedi, P., Craxton, A., Shears, S.B., Tsien, R.Y., Barrett, K.E., Traynor-Kaplan, A. 1994. Long-term uncoupling of chloride secretion from intracellular calcium levels by Ins(3,4,5,6)P_4. *Nature* **371:**711–714

Valdivia, C., Valdivia, H.H., Potter, B.V.L., Coronado, R. 1990. Ca^{2+} release by inositol-trisphosphorothioate in isolated triads of rabbit skeletal muscle. *Biophys. J.* **57:**1233–1243

Valdivia, C., Vaughan, D., Potter, B.V.L., Coronado, R. 1992. Fast release of $^{45}Ca^{++}$-induced by inositol 1,4,5-trisphosphate and Ca^{++} in the sarcoplasmic reticulum of rabbit skeletal muscle: evidence for two types of Ca^{++} release channels. *Biophys. J.* **61:**1184–1193

Vergara, J., Tsien, R.Y., Delay, M. 1985. Inositol 1,4,5-trisphosphate: a possible chemical link in excitation-contraction coupling in muscle. *Proc. Natl. Acad. Sci. USA* **82:**6352–6356

Wilcox, R.A., Challiss, R.A.J., Liu, C., Potter, B.V.L., Nahorski, S.R. 1993. Inositol-1,3,4,5-tetrakisphosphate induces calcium mobilization via the Inositol-1,4,5-trisphosphate receptor in SH-SY5Y neuroblastoma cells. *Mol. Pharmacol.* **44:**810–817

Wu, J.T., Gong, Q.H., Chou, R.H., Wieland, S.J. 1991. Ca^{++}-insensitive modulation of a K^+ conductance by inositol polyphosphates. *J. Biol. Chem.* **266:**14893–14895

Yu, X., Hao, L., Inesi, G. 1994. A pK change of acidic residues contributes to cation countertransport in the Ca-ATPase of sarcoplasmic reticulum. *J. Biol. Chem.* **269:**16656–16661